

Removal of trisacryl red using hydrogels composites based on chitosan

Houari Sebti^{a,b,*}, Nihel Dib^{a,c}, Fatima Zohra Sebba^a, Boumediene Bounaceur^a

^aDépartement de Chimie Laboratoire de Chimie Physique Macromoléculaire, Université Oran1, Oran 31000, Algérie

^bDépartement de la FPST, Ecole Nationale Polytechnique d'Oran, Oran 31000, Algérie

^cEcole Supérieure en Sciences Biologiques d'Oran, Oran 31000, Algérie

Article history:

Received: 20 September 2023 / Received in revised form: 24 November 2023 / Accepted: 3 December 2023

Abstract

This study entails the radical copolymerization synthesis of (2-acrylamido-2-methyl-1-propane sulfonic acid) AMPS, utilizing (N,N'-methylene bis-acrylamide) MBAm as a cross-linking agent and potassium persulfate (PPS) as an initiator to produce chitosan-based composite hydrogels. The investigation involved the various masses of chitosan (250, 500, and 1000 mg). The characterization of the obtained composites and the dye adsorption process was carried out using FTIR, TGA, SEM, UV-visible, and STEM techniques. Swelling properties in distilled water were examined, revealing that the swelling rates at temperatures of 25°C and 37°C for the hydrogel of poly(AMPS-g-MBAm)/chitosan (1000 mg) exceed those of hydrogels with poly(AMPS-g-MBAm)/chitosan (250 and 500 mg). Furthermore, the sorption capacities of the dye were investigated, demonstrating that the sorption capacities of poly (AMPS-g-MBAm)/chitosan (1000 mg) at different temperatures surpass those of poly(AMPS-g-MBAm)/chitosan (250mg, and 500 mg).

Keywords: Composite hydrogels; chitosan; scanning transmission electron microscopy; trisacryl red; swelling behavior; removal dye

1. Introduction

Dyes constitute a broad category of organic chemicals distinguished by their molecular structures, including azo benzene, anthraquinone, or triphenyl methane [1]. These compounds find extensive applications in various industries such as textiles, cosmetics, paper printing, leather, and plastics [2]. Azo compounds, particularly azo dyes, have been recognized for so long as the most widely used class of dyes [3]. Unfortunately, despite their prevalence in the textile and paper industries, azo dyes pose toxicity risks to living organisms [4].

In dyeing processes, sulfates, sulfides, hydrosulfides, and dithionite are commonly employed [5,6]. Today, dyes represent one of the most common pollutants in wastewater [7], and even minute quantities of dyes in water (less than 1 ppm for some dyes) are deemed intolerable [8]. Consequently, numerous methods for dye removal, such as coagulation and flocculation [9], membrane separation [10], oxidation or crowning [11], electro-coagulation [12], and adsorption [13], have been developed.

Over the past decade, adsorption has emerged as an efficient and cost-effective method for removing dyes from wastewater, particularly through the use of new hydrogels like composites exhibiting high sorptive power for dyes [14]. Chitosan, a natural polysaccharide, has been widely utilized for crafting biocompatible hydrogels [15]. The growing interest in polysaccharide hydrogels is evident, with frequent applications as wound dressings [16]. The pH-responsive nature of chitosan, attributed to its amine groups [17], enhances its adaptability to

various conditions.

Chitosan's exceptional qualities, including its affinity for metals, proteins, and dyes, coupled with its biocompatibility, biodegradability, hydrophilicity, non-toxicity, cationicity, ease of modification, and ability to form gels, films, nanoparticles, and microparticles, contribute to its widespread use [18]. Notably, Ag nanocomposite microporous hydrogels and P(AAm-co-NVP)/Chitosan/Chitosan exhibit different swelling ratios. For P(AAm-co-NVP)/Chitosan and P(AAm-co-NVP)/CS-Ag, the resulting swelling ratios range from 14.5 to 22.5 and 4.5 to 6, respectively [19]. Chitosan hydrogels produced by physical cross-linking demonstrate high water absorption, with equilibrium water content values between 23 and 30 times their mass [20].

Hydrogels, characterized by their capacity to absorb and retain the substantial amounts of water, undergo swelling when exposed to solutions containing dye molecules. This swelling process, typically reversible, is determined by various factors, including pH, temperature, and the polymer type [21].

The adsorption of dye by hydrogels demonstrates an increase corresponding to the enhanced swelling behavior. As the swelling behavior of the hydrogels increases, so does their capacity to adsorb dye molecules." This rephrasing makes it explicit that there is a positive correlation between the swelling behavior of the hydrogels and their ability to adsorb dye [22].

2. Materials and Methods

2.1. Materials

2-acrylamido-2-methyl-1-propane sulfonic acid (AMPS), N,N'-methylene bis-acrylamide (MBAm) (Sigma-Aldrich, USA), initiator Potassium persulfate (PPS), chitosan (Sigma-

* Corresponding author.

Email: sebti.houari@yahoo.fr

<https://doi.org/10.21924/cst.8.2.2023.1278>

Aldrich, USA), solvent Methanol (Shanghai Chemical Group, China).

The samples were analyzed using FTIR spectroscope IFS66in the region of 4000–400cm⁻¹ Bruker, (Ettlingen, Germany). Prior to the measurement, the samples were dried under vacuum until reaching a constant weight. The dried samples were pressed into the powder, mixed with 10 times as much KBr powder, and compressed to make a pellet for FTIR characterization.

The chemical was detected using Thermoquest Elemental Analyzer NA 2500 (Thermo Finnigan) United Kingdom. It was coupled with Cathetometer data management (Eager 200 software) as assayed elements are C, H, N, S and O. The results were validated for two minimum tests. UV-visible spectrophotometer (Spectronic Genesys, USA) with a wavelength of 200 to 1100 nm was used to measure trisacryl red. Scanning electron microscopy (SEM) was used to investigate the morphology of the prepared hydrogel. Measurements were taken on a (Zeiss Sigma 982) Germany with an acceleration of 20kV. Scanning transmission electron microscopy (Thermo Scientific Talos F200X (S), USA) with TEM resolution Limit of 0.16 nm (in High-Angle Annular Dark Field–HAADF mode) was used to visualize the structure and composition.

2.2 Methods

2.2.1. Synthesis of poly (AMPS-g-MBAm) / Chitosan hydrogels

Hydrogels composing of poly(2-Acrylamido-2-Methyl-1-propane sulfonic Acid (AMPS)-g-N,N' methylene bis-acrylamide (MBAm)/Chitosan at 250, 500, and 1000 mg were synthesized using the radical polymerization technique in distilled water.

For the preparation of hydrogels, a solution comprising 2 g of (AMPS) and 165 mg of (MBAm) with 102 mg of thermal decomposition of potassium persulfate was dispersed in 10 ml of distilled water. The reaction was conducted at 60 °C under an inert atmosphere for 4 hours, 3 hours, and 2 hours, respectively, for the different mass chitosan.

The resulting products underwent purification three times using distilled water with magnetic stirring, followed by an additional three purifications with ethanol. The purified hydrogels were initially dried at room temperature for 24 hours and further dried at the temperature of 60°C. Experimental conditions are detailed in Table 1.

2.2.2. Swelling behavior of poly (AMPS-g-MBAm)/Chitosan hydrogels

The swelling behavior of hydrogels was investigated at various temperatures. Each dried hydrogel was placed in a 20 ml screw-capped glass vial, to which 10 ml of distilled water [14] was added, and shaken at room temperature for 24 hours. The hydrogels were periodically removed from the solution,

blotted with wax paper, and the swelling ratio was calculated by weighing the hydrogels using the formula

$$SR = \frac{W_{hs}}{W_{hd}} \quad (1)$$

w_{hs} indicates the mass of swelling at a predetermined time interval, and w_{hd} represents the weight of dried gel before starting of swelling experiments.

2.2.3 Sorption experiments

All adsorption tests were performed by the batch method by adding 50 mg of hydrogel composite into a flask containing 10 mL trisacryl red solution, shaking at 200 rpm. The initial concentrations of trisacryl red (5–20 ppm), and temperature (25°C–37°C) were varied to study the effects of adsorption parameters. The initial pH of trisacryl red solution was adjusted to neutral pH = 6.5. At desired time intervals, the remaining trisacryl red concentrations were measured by UV–vis spectrophotometer (Lambda at 650 nm). After sampling, the volume of the remaining trisacryl red solution in the flask was adjusted to 10 ml. The adsorption capacity as a function of time (q_t (mg/g) and the adsorption capacity at equilibrium (q_e ; mg/g) were determined by Eq. (1) and (2), respectively. The dye removal efficiency, $R\%$, was expressed as a percentage as follows (Eq. (3))

$$q_t = \frac{(c_0 - c_t) \cdot V}{m} \quad (2)$$

$$q_e = \frac{(c_0 - c_e) \cdot V}{m} \quad (3)$$

$$\%R = \frac{c_0 - c_e}{c_0} \quad (4)$$

where C_0 , C_t and C_e (mg/L) are the initial, given time, and equilibrium concentrations of trisacryl red, respectively, V (l) is the solution volume, and m (g) is the adsorbent mass [23].

3. Results and Discussion

3.1 FTIR study

Test condition: A background spectrum should be collected using a clean sample holder (KBr pellet) without any sample. This background spectrum helped to correct for contributions from the environment. FTIR analysis aimed to determine the functional groups present in various starting materials, as illustrated in Figure 1. The band at 3288 cm⁻¹ was assigned to the O-H group, indicating the presence of AMPS, as well as the N-H group of MBAm and chitosan, the band in Figure C was more intense compared to Figures a and b. This confirmed that the intensity of the band was proportional to the mass ratio of chitosan. The carbonyl group adsorption band of the C=O ester function (MBAm) is

Table 1. Experimental conditions of radical copolymerization (solvent: distilled water, temperature 60 °C and PPS)

Hydrogels	AMPS mg	MBAm mg	Chitosan mg	PPS mg	distilled water ml	T °C	t (h)
poly (AMPS-g-MBAm)/Chitosan	2000	165	250	102	10	60	4
			500				3
			1000				2

observed at 1635 cm^{-1} . The valence vibration bands at 1140 and 1101 cm^{-1} corresponded to the functional group C-N of (MBAm, AMPS) and the S-O functional group of AMPS. Additionally, an absorption band at 1080 and 1015 cm^{-1} corresponded to the C-O-C and C-O-H cyclic bonds of chitosan.

3.2. Thermal analysis

Test condition: Hydrogel samples should be prepared consistently with excess water removed by air-drying the samples. This ensured that the TGA results primarily reflected the composition of the hydrogel. An appropriate heating rate was based on the expected decomposition or degradation of the hydrogel. A commonly used heating rate is 5 $^{\circ}\text{C}/\text{min}$.

Figure 2 depicts the thermal analysis of poly(AMPS-g-MBAm) modified by different percentages of chitosan. All samples underwent three stages of degradation, with the first occurring between 73 $^{\circ}\text{C}$ and 100 $^{\circ}\text{C}$. This was primarily attributed to the physisorbed water on the surface of these

hydrogels, highlighting their hydrophilic nature. For hydrogel 250 mg, hydrogel 500 mg, and hydrogel 1000 mg, mass losses were estimated at 10%, 4%, and 3%, respectively.

In the second step, the degradation of specific functional groups within the hydrogel composites resulted in the mass losses of about 20%, 11%, and 10% for hydrogel 250 mg chitosan, hydrogel 500 mg chitosan, and hydrogel 1000 mg chitosan, respectively, occurred from 130 $^{\circ}\text{C}$ to 230 $^{\circ}\text{C}$.

In the third step, a total degradation of composite hydrogels was observed for all three products with a mass loss of about 80% for poly (AMPS-g-MBAm)/chitosan 250 mg from 260 $^{\circ}\text{C}$ to 320 $^{\circ}\text{C}$. Similarly, in the third stage, hydrogel poly(AMPS-g-MBAm)/chitosan 500 mg showed total degradation between 260 $^{\circ}\text{C}$ and 330 $^{\circ}\text{C}$, losing approximately 72% of its mass. The third stage for poly(AMPS-g-MBAm)/chitosan 1000 mg exhibited total degradation from 260 $^{\circ}\text{C}$ to 330 $^{\circ}\text{C}$ with a mass loss of approximately 71%. We observed that the mass loss relative to temperature is as follows: 1.2 mg for poly (AMPS-g-MBAm)/1000 mg chitosan, 1.3 mg for poly (AMPS-g-MBAm)/500 mg chitosan, and 1.45 mg for poly

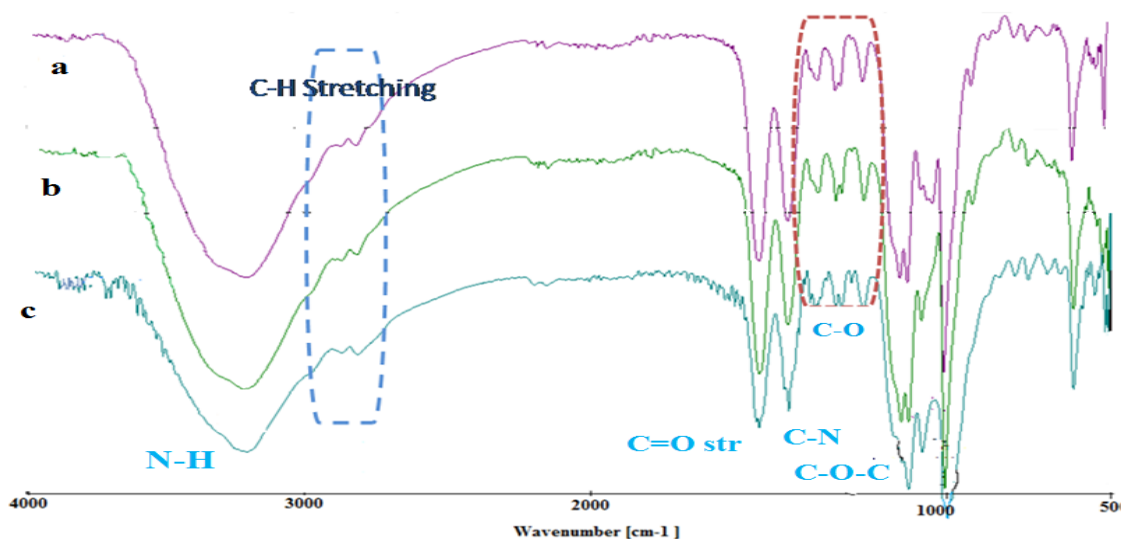


Fig. 1. FTIR spectra of hydrogels composites by varying the mass of chitosan: (a) poly (AMPS-g-MBAm)/ 250 mg chitosan, (b) poly (AMPS-g-MBAm)/ 500 mg chitosan, (c) poly (AMPS-g-MBAm)/ 1000 mg chitosan

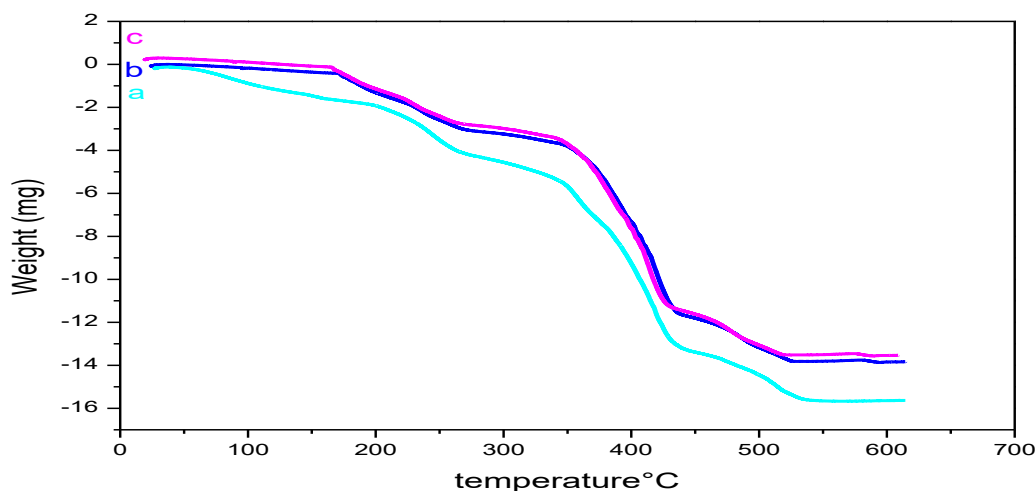


Fig. 2. Thermogravimetric analysis of hydrogels composites by varying the mass of chitosan. (a) poly (AMPS-g-MBAm)/ 250mg chitosan, (b) poly (AMPS-g-MBAm)/ 500 mg chitosan, (c) poly (AMPS-g-MBAm)/ 1000mg chitosan

(AMPS-g-MBAm)/250 mg chitosan, respectively. These results con-confirmed the increasingly important role of chitosan incorporation within the hydrogel to thermally stabilize the material.

3.3. Swelling behavior of the poly (AMPS-g-MBAm)/Chitosan hydrogels.

The equilibrium swelling ratios in distilled water at 25 °C and 37 °C (Table 2) showed a proportional relationship to the mass ratios of chitosan incorporated into each hydrogel. The observed trend suggested that the incorporation of chitosan played a significant role in extending the network, potentially determining the swelling behavior. There was evidence of a two-step diffusion process (Figure 3 and Figure 4). The first step involved fast diffusion linked to the absorption of the solvent within hydrogels, reaching both more and less accessible sites of chitosan functional groups. The second step included the adsorption of the solvent by hydrogel surfaces, driven by physical interactions like hydrogen bonds.

Table 2. Equilibrium weight swelling rate of poly (AMPS-g-MBAm)/chitosan (250, 500 and 1000 mg) hydrogels, (T=25°C, T=37°C; m=20 mg) in distilled water

Hydrogels	Chitosan (mg)	Temperature (°C)	Swelling ratio
Poly(AMPS-g-MBAm)	250	25	27
		37	39
	500	25	47
		37	50
	1000	25	53
		37	59

Swelling ratio values are presented as a function of temperature at equilibrium (Figure 5). The swelling ratios at 37°C were found higher than that of 25°C. The observed values at both temperatures were proportional to the mass ratios of chitosan, suggesting that the amount of chitosan influenced the swelling behavior.

These findings collectively indicated that the incorporation of chitosan into hydrogels had a notable impact on their swelling behavior. Additionally, the temperature dependency of swelling ratios further suggested that temperature played a role in this phenomenon with higher temperatures leading to increased swelling. The two-step diffusion process described provided insights into the mechanisms involved in the absorption of the solvent within the hydrogels.

At a temperature of 20°C, it is noted that materials with chitosan amounts of 500 and 1000 mg exhibited SR values that were nearly identical and significantly different from the material with 250 mg of chitosan. This suggested that at this lower temperature, the influence of chitosan mass on the swelling rate dominated over the temperature effect. The higher masses of chitosan (500 and 1000 mg) led to similar SR values, possibly indicating a saturation point where additional chitosan did not significantly impact the swelling rate further. Meanwhile, the material with 250 mg of chitosan differed significantly, emphasizing the role of chitosan mass at this specific temperature.

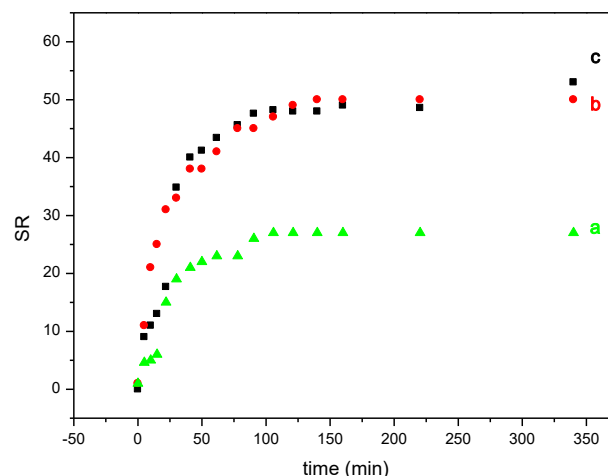


Fig. 3. swelling behavior by hydrogels composites T=25°C, (a) poly (AMPS-g-MBAm)/ 250mg chitosan, (b) poly (AMPS-g-MBAm)/ 500 mg chitosan, (c) poly (AMPS-g-MBAm)/ 1000mg chitosan

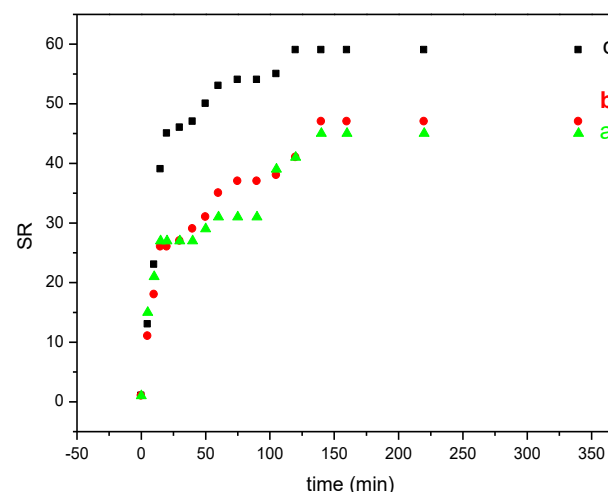


Fig. 4. swelling behavior by hydrogels composites T=37°C, (a) poly (AMPS-g-MBAm)/ 250mg chitosan, (b) poly (AMPS-g-MBAm)/ 500 mg chitosan, (c) poly (AMPS-g-MBAm)/ 1000mg chitosan

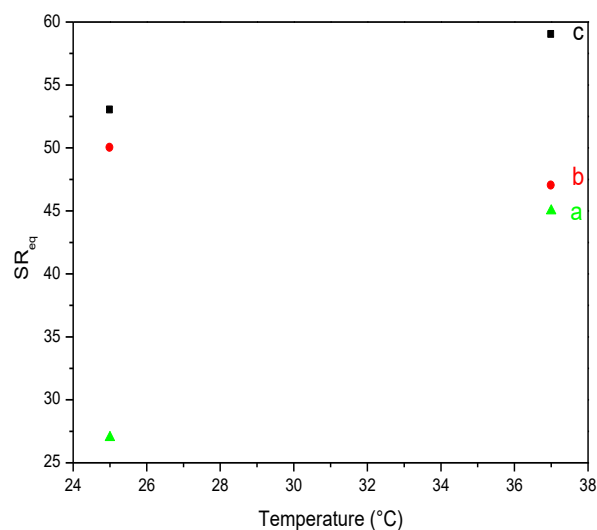


Fig. 5. swelling behavior as a function of temperature swelling behavior as a function of temperature. (a) poly (AMPS-g-MBAm)/ 250mg chitosan, (b) poly (AMPS-g-MBAm)/ 500 mg chitosan (c) poly (AMPS-g-MBAm)/ 1000mg chitosan

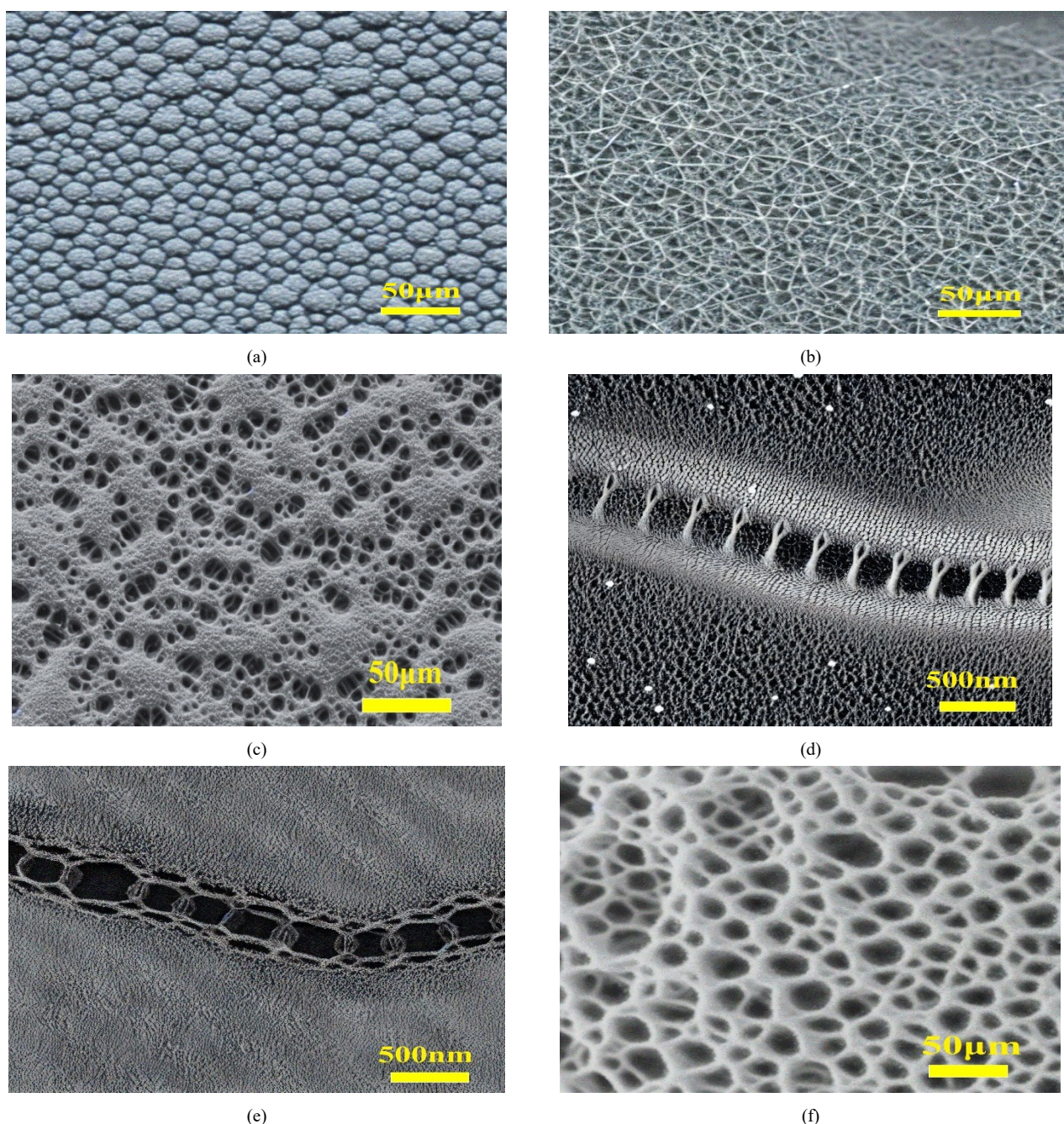


Fig. 6. SEM image of obtained samples. (a) Chitosan, (b) poly (AMPS-g-MBAm)/ 250 mg chitosan, (c and d) poly (AMPS-g-MBAm)/ 500 mg chitosan, (e and f) poly (AMPS-g-MBAm)/1000 mg chitosan

On the other hand, at a higher temperature of 37°C, the situation shifted. Materials with 250 and 500 mg of chitosan displayed almost identical SR values, indicating that the temperature effect was more prominent in this range, potentially accelerating the swelling rate. The material with 1000 mg of chitosan, however, differed significantly, suggesting that at this higher temperature, the mass of chitosan started to play a more crucial role. The material with 1000 mg of chitosan might experience a different interaction with temperature, leading to a distinct SR value compared to the other masses.

3.4. Scanning electron microscopy (SEM)

Test condition: Dependent upon the nature of the hydrogel, fixation may be necessary to preserve the structure. Common

fixatives include glutaraldehyde or formaldehyde. Hydrogels typically contain a significant amount of water, which needs to be removed before SEM analysis. Gradual dehydration using a series of ethanol solutions of increasing concentration is a common approach.

The morphology of the composite materials was investigated through SEM images. Figure 6 presents the SEM images of various samples at different magnifications (Figure 6(a)). Notably, the surface of chitosan appeared granulated rather than porous. In the image of poly (AMPS-g-MBAm)/chitosan 250 mg (Figure 6(b)), entangled irregular fibers constituted the porous matrix of the hydrogel.

Porous microstructures were observed in the poly (AMPS-g-MBAm)/chitosan hydrogel formulations of 500 mg (Figure 6(c) and Figure 6(d)) and 1000 mg (Figure 6(e) and Figure 6(f)), suggesting that these hydrogels were formed through cross-

linking AMPS and MBAm groups. Additionally, the introduction of additives (chitosan) seemed to determine the porosity of the hydrogels. The change in mean pore size with the incorporation of chitosan indicated its impact on the polymer network structure.

Moreover, the average pore diameter was measured as 3 μm , 7 μm , and 15 μm for poly(AMPS-g-MBAm)/chitosan 250 mg, 500 mg, and 1000 mg, respectively. This finding aligned with the earlier results obtained during the determination of swelling ratios [24,25,26], confirming that the presence of chitosan significantly affected the hydrogel's structure and properties. The results obtained are summarized in Table 3.

Table.3. The particle sizes of hydrogels composites obtained through scanning electron microscope (SEM) analysis for three different variations

Products	Figure 6	Particle Sizes	Pore Sizes
Chitosan	Fig. 6(a)	50 μm	-
poly (AMPS-g-MBAm)/ 250 mg chitosan	Fig. 6(b)	50 μm	3 μm
poly (AMPS-g-MBAm)/ 500 mg chitosan	Fig. 6(c)	50 μm	7 μm
poly (AMPS-g-MBAm)/ 1000 mg chitosan	Fig. 6(d)	500 nm	15 μm

4. Sorption experiments

The curves depicting variations in the sorption capacities of the dye (5 ppm and 20 ppm) by the hydrogels of poly(AMPS-g-MBAm)/chitosan at the temperatures of 25 and 37°C (Figure 7 and Table 4) illustrate two distinct sorption stages. In the initial stage, there was a gradual diffusion of the dye through the hydrogel, leading to an increase in sorption capacity. The results suggested that the absorption process during this phase was not primarily governed by electrostatic interactions. In this particular scenario, the surface of the obtained hydrogel of poly(AMPS-g-MBAm)/1000 mg exhibited a significant presence of amino groups ($-\text{NH}_2$) and hydroxyl groups ($-\text{OH}$). These functional groups were advantageous for facilitating hydrogen bonding between the hydrogel and dyes. Consequently, hydrogen bonding emerged as the predominant mechanism influencing the absorption process during the first stage.

Following the initial stage, a second stage was observed wherein the hydrogel reached saturation, corresponding to the equilibrium capacity value. In this stage, the results indicated that the absorption process was dominated by electrostatic interactions. Regardless of the temperature, the sorption capacity showed a proportional increase with the chitosan level. This suggested that the incorporation of chitosan positively determined the sorption capacity of the hydrogel.

These results were in good agreement with those observed when studying the swelling ratios. This new phrase has made it clear that there was a positive correlation between the hydrogels' swelling behavior and their capacity to adsorb dye molecules: As the hydrogels' swelling behavior increases, so does their capacity to adsorb dye molecules. In hydrogel based chitosan system, the relationship between sorption capacity and removal efficiency is a crucial aspect in understanding the performance of these materials in various applications, particularly in water treatment and environmental remediation. The relationship between sorption capacity and removal

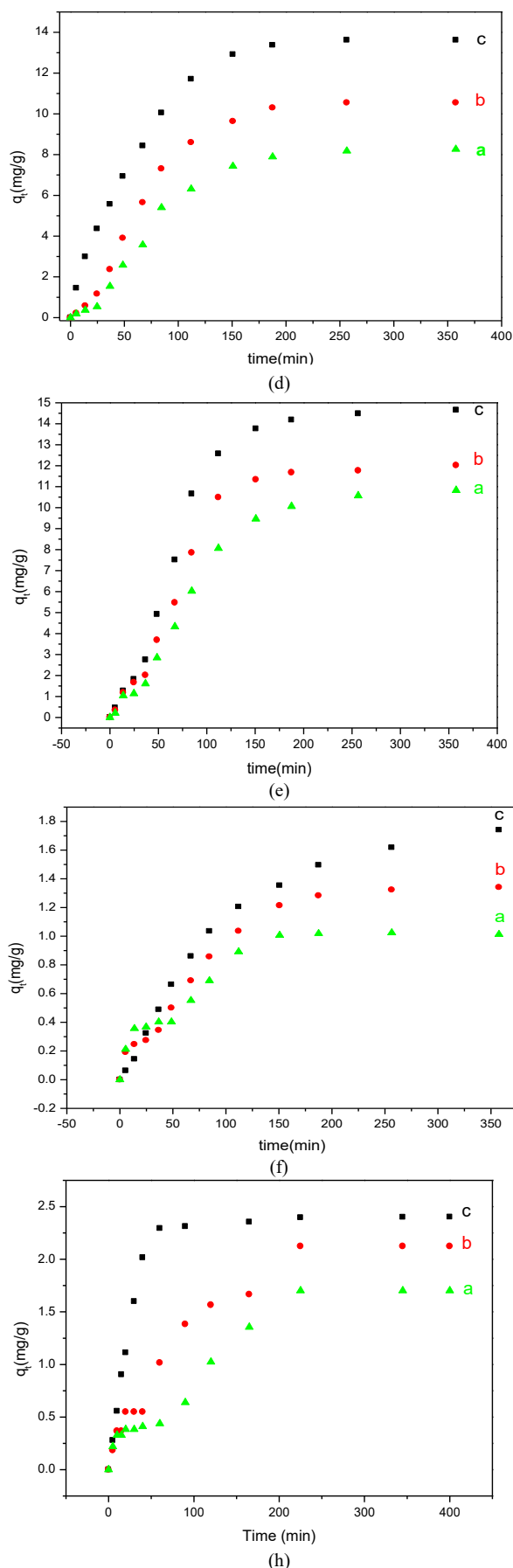
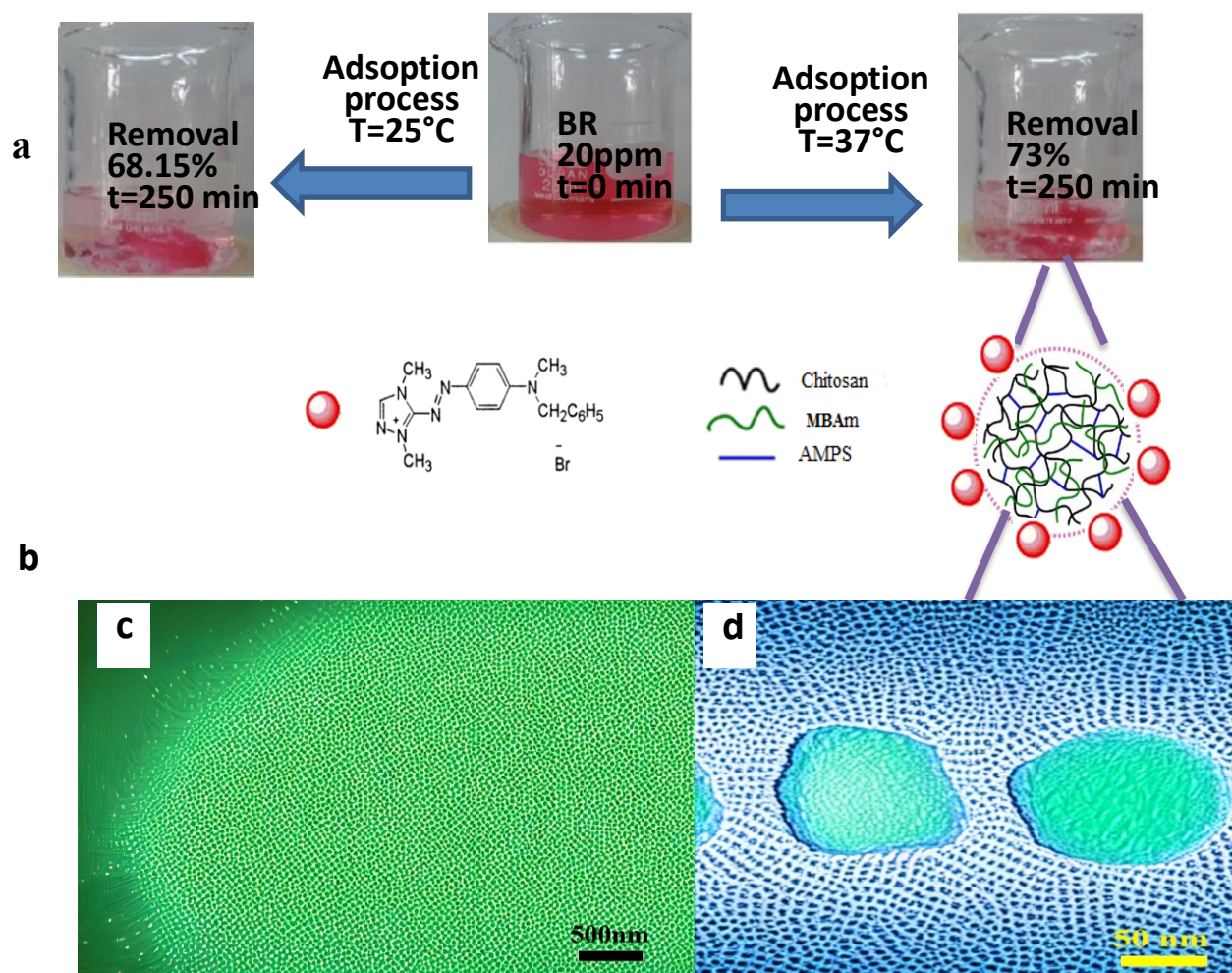


Fig.7. adsorption capacity of dye by hydrogels composites as a function of time (d) 20ppm, T=25°C; (e) 20ppm T=37°C, (f) 5ppm, T=25°C; (h) 5ppm, T=37°C. (a) poly (AMPS-g-MBAm)/ 250mg chitosan, (b) poly (AMPS-g-MBAm)/ 500 mg chitosan, (c) poly (AMPS-g-MBAm)/ 1000mg chitosan

Table 4. The equilibrium sorption capacities and removal efficiency of the dye by hydrogels of poly (AMPS-g-MBAm)/chitosan in distilled water, initial concentration of the dye $C_0=5\text{mg/l}$ and $C_0=20\text{mg/l}$ at $T=25^\circ\text{C}$, $T=37^\circ\text{C}$.

Hydrogel	Chitosan (mg)	T ($^\circ\text{C}$)	q_{eq} (mg/g)		Removal efficiency (%)	
			$C_0=5\text{mg/l}$	$C_0=20\text{mg/l}$	$C_0=5\text{mg/l}$	$C_0=20\text{mg/l}$
Poly (AMPS-g-MBAm)	250	25	1.01	8.40	20.20	42
		37	1.70	10.31	34	51.55
	500	25	1.34	10.12	26.80	51
		37	2.12	12.08	42.40	60.40
	1000	25	1.64	13.63	32.80	68.15
		37	2.40	14.60	48	73

Fig. 8. Schematic illustration of the poly (AMPS-g-MBAm)/chitosan 1000 mg composite hydrogel at 37°C (a) adsorption process, (b) STEM depicts the adsorption process at the start and in equilibrium

efficiency is often direct. A higher sorption capacity generally leads to higher removal efficiency. If the hydrogel has a greater ability to adsorb or absorb the target substance, it can effectively reduce the concentration of that substance in the solution, resulting in higher removal efficiency. However, other factors also influence removal efficiency, such as temperature, and the initial concentration of the dye. The design and composition of the hydrogel, including chitosan mass and structural characteristics, play a crucial role in determining sorption capacity and, consequently, removal efficiency.

FTIR can identify specific functional groups on the surface

of a material. These functional groups play a crucial role in sorption interactions. For example, hydroxyl ($-\text{OH}$), amino ($-\text{NH}_2$), and carboxyl ($-\text{COOH}$) groups are common functional groups in sorbent materials. Correlating the presence or absence of specific functional groups with sorption capacity can reveal the types of interactions involved in the adsorption process.

According to scanning electron microscopy and sorption capacity, we noticed the following key points. Larger pores in hydrogels can facilitate the easy entry of dye molecules into the internal structure of the hydrogel. Smaller pores may limit the accessibility of dye molecules, affecting the overall adsorption

capacity. Generally, hydrogels with larger pore sizes tend to have a greater surface area available for adsorption. A larger surface area provides more sites for dye molecules to interact and be adsorbed onto the hydrogel.

TGA of chitosan-based hydrogels provides valuable information about their thermal behavior, composition, and structural changes during different temperature ranges. Correlating TGA data with sorption capacity measurements

allows for a comprehensive understanding of the interplay between the hydrogel's thermal characteristics and its performance in sorption applications. This information is useful for optimizing hydrogel formulations for specific sorption requirements, such as environmental remediation or biomedical applications.

The adsorption capacity values were validated by Figure 8. In Part a, the adsorption process before and after adsorption for poly(AMPS-g-MBAm)/chitosan 1000 mg resulted in the yields of 73% and 68% at 250 min at temperatures of 37°C and 25°C, respectively. STEM image Part b shows dye adsorption by poly(AMPS-g-MBAm)/1000 mg chitosan at 37°C. In STEM image (d) depicting dye adsorption at 5 minutes, we observed a multilayer physical adsorption of dye on the hydrogel surface. STEM image (c) illustrating dye adsorption at equilibrium showed the distribution of dye across the entire hydrogel surface. These findings were well-aligned with the observations made during the examination of swelling ratios.

5. Conclusion

The composites poly (AMPS-g-MBAm)/Chitosan were successfully synthesized through radical polymerization. The SEM analysis of the composite materials distinctly revealed that an increase in chitosan content resulted in the formation of a porous structure. When chitosan was incorporated into the hydrogel, there is a noticeable change in the mean pore size, indicating the significant impact of chitosan on the polymer network structure. Thermogravimetric analysis further supported the growing importance of chitosan incorporation within the hydrogel, emphasizing its role in enhancing thermal stability. The swelling ratio values in distilled water at 25°C and 37°C exhibited a direct proportionality to the mass ratios of chitosan. The considerable equilibrium swelling rates of the hydrogels affirmed their superabsorbent. Moreover, the high performance of the obtained composites was assessed in the reduction of organic pollutants at various temperatures. The adsorption capacity values aligned with those observed in the study of swelling ratios, reinforcing the consistent behavior of the composites across different evaluations. These results collectively underscored the versatile and advantageous properties of the poly (AMPS-g-MBAm)/Chitosan composites, positioning them as promising materials for applications in pollutant reduction and other relevant fields.

References

1. A.Z.M. Badruddoza, G.S.S Hazel, K. Hidajat and K.M.S. Uddin, *Synthesis of carboxymethyl- β -cyclodextrin conjugated magnetic nano-adsorbent for removal of methylene blue*, Colloids Surf. A Physicochem. Eng. Asp. 367 (2010) 85–95.
2. N.K. Goel, V. Kumar, S. Pahan, Y. K hardwaj and S. Sabharwal, *Development of adsorbent from Teflon waste by radiation induced grafting: Equilibrium and kinetic adsorption of dyes*, J. Hazard. Mater, 193 (2011) 17–26.
3. H.F. Rizk, A. Ibrahim and A.M. El-Borai, *Synthesis, dyeing performance on polyester fiber and antimicrobial studies of some novel pyrazolotriazine and pyrazolyl pyrazolone azo dyes*, Arab. J. Chem, 10 (2017) S3303–S3309.
4. P. Rajaguru, L. Vidya, B. Baskarase thupathi, P.A. Kumar, M. Palanivel and K. Kalaiselvi, *Genotoxicity evaluation of polluted ground water in human peripheral blood lymphocytes using the comet assay*, Mutat. Res. 517 (2002) 29–37.
5. F.P. Vander Zee I.A.E. Bisschops, V.G. Blanchard R.H.M. Bouwman, G. Lettinga and J.A. Field, *The contribution of biotic and abiotic processes during azo dye reduction in anaerobic sludge*, Water Res. 37 (2003) 3098–3109.
6. K. Rasool, A. Shahzad and D.S. Lee, *Exploring the potential of anaerobic sulfate reduction process intreating sulfonated diazo dye: Microbial community analysis using bar-coded pyro sequencing*, J. Hazard. Mater. 318 (2016) 641–649.
7. V.V. Panic and S.J. Velickovic, *Removal of model cationic dye by adsorption onto poly (methacrylic acid)/zeolite hydrogel composites: Kinetics, equilibrium study and image analysis*, Sep. Purif. Technol. 122 (2014) 384–394.
8. S. Chen, J. Zhang, C. Zhang, Q. Yue, Y. Li and C. Li, *Equilibrium and kinetic studies of methyl orange and methyl violet adsorption on activated carbon derived from Phragmites australis*, Desalination. 252 (2010) 149–156.
9. S. Sadri Moghaddam, M.R. Alavi Moghaddam and M. Arami, *Coagulation/flocculation process for dye removal using sludge from water treatment plant: Optimization through response surface methodology*, J. Hazard. Mater. 175 (2010) 651–657
10. A. Szygula, E. Guibal, M.A. Palacin, M. Ruiz and A.M. Sastre, *Removal of an anionic dye (Acid Blue 92) by coagulation flocculation using chitosan*, J. Environ. Manage., 90, (2009) 2979–2986.
11. G. Ciardelli, L. Corsi and M. Marcucci, *Membrane separation for wastewater reuse in the textile industry*. Resour. Conserv. Recy. 31 (2001) 189–197.
12. M. Muthukumar and N. Selvakumar, *Studies on the effect of inorganic salts on decolouration of acid dye effluents by ozonation*, Dyes Pigm, 62 (2004) 221–228.
13. A. Alinsafi, M. Khemis, M.N. Pons, J.P. Leclerc, A. Yaacoubi, A. Benhammou and A. Nejmeddine, *Electro-coagulation of reactive textile dyes and textile wastewater*, Chem. Eng. Process. 44 (2005) 461–470.
14. M.U. Dural, L. Cavas, S.K. Papageorgiou and F.K. Katsaros, *Methylene blue adsorption on activated carbon prepared from Posidonia oceanica (L.) dead leaves: Kinetics and equilibrium studies*, Chem. Eng. J. 168 (2011) 77–85.
15. X. Vecino, D. Rey, J.M. Cruz and A.B. Moldes, *Study of the physical properties of calcium alginate hydrogel beads containing vineyard pruning waste for dye removal*, Carbohydr. Polym, 115 (2015) 129–138.
16. M. He, B. Han, Z. Jiang, Y. Yang, Y. Peng, and W. Liu, *Synthesis of a chitosan-based photo-sensitive hydrogel and its biocompatibility and biodegradability*, Carbohydr. Polym, 166 (2017) 228–235.
17. E.M. Ahmed, *Hydrogel: Preparation, characterization, and applications: A review A revi*, J. Adv. Res, 6 (2015) 105–121.
18. M. Pieróg, M. Gierszewska-Dróżyńska and J. Ostrowska-Czubenko, *Effect of Ionic Cross-Linking Agents on Swelling Behavior of Chitosan Hydrogel Membranes*, Prog. Chem. Appl. Chitin. Deriv. XIV (2009) 75–82.
19. S. Rehmani, M. Ahmad, M. Usman Minhas, H. Anwar and M. Imad-ud-din Zangi, Sohail, *Development of natural and synthetic polymer-based semi-interpenetrating polymer network for controlled drug delivery: optimization and in vitro evaluation studies optimization and in vitro evaluation studies*, Polym. Bull. 74 (2016) 737–761.
20. F. V Gabriela, H.E. Andrews, J. M. Cervantes, G.L. Bárcenas, M. V. Lepe, N. M. Hernández, J. A. Jiménez-Ávalos, D. G. Mejía-Torres, P. Ramos-Martínez and R. Rodríguez-Rodríguez, *Porous Chitosan Hydrogels Produced by Physical Crosslinking: Physicochemical, Structural, and Cytotoxic Properties*, Polym. 15 (2023) 1–15.
21. S. A. Malik, A. A. Dar and J. A. Banday, *Rheological, morphological and swelling properties of dysprosium-based composite hydrogel beads of alginate and chitosan: A promising material for the effective cationic and anionic dye removal*, Colloids. Surf. A Physicochem. Eng. Asp, 663 2023.
22. N. F. Alharby, R. S. Almutairi, and Nadia A. Mohamed, *Adsorption Behavior of Methylene Blue Dye by Novel CrossLinked O-CM-Chitosan Hydrogel in Aqueous Solution: Kinetics, Isotherm and Thermodynamics*,

- Polym. 13 (2021) 1-28
23. M. Srikaew, P. Jumpapaeng, P. Suwanakood, C. Kaiyasuan, V. Promarak and S. Saengsuwan, *Rapid synthesis and optimization of UV-photopolymerized cassava starch-based superabsorbent hydrogels as a biodegradable, low-cost and effective adsorbent for MB removal*, J. Ind. Eng. Chem. 118 2023 53-69
24. M. Rinaudo, *Chitin and chitosan: Properties and applications*, Prog. Polym Sci. 31 (2006) 603–632.
25. S. Jin, F. Bian, M. Liu, S. Chen, S, and H. Liu, H, *Swelling mechanism of porous P(VP-co-MAA)/PNIPAM semi-IPN hydrogels with various pore sizes prepared by a freeze treatment*, Polym. Int. 2009 58 142–148.
26. A. Demba N'diaye, M. Sid'Ahmed Kankou, B. Hammouti, A. B. D. Nandiyanto and D. F. Al Husaeni, *A review of biomaterial as an adsorbent: From the bibliometric literature review, the definition of dyes and adsorbent, the adsorption phenomena and isotherm models, factors affecting the adsorption process, to the use of typha species waste as a low-cost adsorbent*, Commun. Sci. Technol. 7 (2) (2022) 140–153.